BNL--44648

DE91 007551

STUDIES OF FREQUENCY DEPENDENT C-V CHARACTERISTICS OF NEUTRON IRRADIATED p^+-n SILICON DETECTORS*

Zheng Li and H. W. Kraner

Brookhaven National Laboratory, Upton, NY 11973

October 1990

***This research was supported by the U. S. Department of Energy: Contract No. DE-AC02-76CH00016.**

DISCLAIMER

Studies of Frequency Dependent C-V Characteristics of Neutron Irradiated p^+-n Silicon Detectors*

Zheng Li and H.W. Kraner
Brookhaven National Laboratory, Upton, NY 11973

Abstract

Frequency-dependent capacitance-voltage fluence (C-V) characteristics of neutron irradiated high resistivity silicon p^+-n detectors have been observed up to a fluence of 8.0×10^{12} n/cm^2. It has been found that frequency dependence of the deviation of the C-V characteristic (from its normal $V^{-1/2}$ dependence), is strongly dependent on the ratio of the defect density and the effective doping density N_t/N_d'. As the defect density approaches the effective dopant density, or $N_t/N_d' \rightarrow 1$, the junction capacitance eventually assumes the value of the detector geometry capacitance at high frequencies ($f \geq 10^5$ Hz), independent of voltage. A two-trap-level model using the concept of quasi-fermi levels has been developed, which predicts both the effects of C-V frequency dependence and dopant compensation observed in this study.

I. INTRODUCTION

It has been well established that as little as 10^{11} n/cm^2 of neutron exposure causes severe degradation in leakage current to the silicon detectors [1-4]. Leakage current degradation has been found to be nearly independent of resistivity over more than three orders of magnitude of silicon resistivities [1]. Although the effect of frequency-dependent capacitance-voltage (C-V) characteristics has been observed on neutron damaged ($\phi_n \geq 10^{15}$ n/cm^2) [5] and Au-doped low resistivity silicon (<5 Ωcm) or $N_d \geq 10^{15}$cm^3) p^+-n junction devices [6] and neutron irradiated high-purity germanium detectors [7], little has been learned about this effect on high resistivity silicon material from which silicon detectors are constructed. A typical value of doping density N_d in silicon used for a silicon detector is of the order of 10^{12} cm^3, giving 5 kΩ-cm resistivity for n-type silicon. If we speculate that a frequency-dependent C-V effect can be observed when $\phi_n/N_d \sim 1$ cm, this would lead to a fluence of ~ 10^{12} n/cm^2, which is just the annual fluence expected for the SSC's initial luminosity of 10^{33}/cm^2-s [8]. It is therefore possible that, in addition to the leakage current degradation, C-V characteristics of the detectors may also change in the SSC experimental environment. This change in C-V characteristics, which will be described in this work, results from changes of detector material parameters such as effective dopant density (or dopant compensation and type inversion) and defect concentration, which are in turn closely related to the detector electrical properties. Thus, it can also be used as a tool to monitor the changes of detector parameters caused by exposure to neutron, proton, or electron radiations.

II. EXPERIMENTAL

The silicon p^+-n junction detectors used in this study were made on n-type <111> wafers, with resistivities ranging from 10 Ω-cm to 10 kΩ-cm. Fast neutrons from 10 keV to 2.2 MeV were obtained from the ^{7}Li(p,n) reaction using 4 MeV protons from a van de Graaff accelerator at the University of Lowell, with the flux of about 4.5×10^8 n/cm^2 -sec. Various groups of detectors were exposed to neutron radiation up to the fluence of 8×10^{12} n/cm^2.

III. RESULTS and DISCUSSION

As it is seen in Fig. 1a, the detector C-V characteristics are frequency independent up to the neutron fluence of 7×10^{10} n/cm^2, which is in a good agreement with the data presented by Vismara [9]. Figure 1b shows the frequency-dependent C-V curves after the detector was exposed to a neutron fluence of 8×10^{12} n/cm^2. At this fluence, the detector high-frequency (f > 50 kHz) C-V characteristics become essentially bias-independent, equaling the detector geometrical capacitance, $\varepsilon\varepsilon_0/d_{Si}$ • Area. It is interesting to note that the full depletion voltage over the entire wafer thickness, d_{Si} = 300 μm in this case, has been reduced from about $V_d = 60$ volts to about 20 volts, indicating a nearly 60% dopant compensation.

Figure 2 shows the values of capacitance at a given voltage as a function of measuring frequency C(f), with neutron fluence ϕ_n being the parameter. It is clear that the degree of the dependence of capacitance on frequency is affected strongly by neutron fluence ϕ_n. Since the ratio of defect concentration and dopant concentration N_t/N_d is proportional to ϕ_n (for $\phi_n \leq 10^{13}$ n/cm^3), one can conclude that this degree of frequency dependence is strongly dependent on N_t/N_d. This argument is supported by the data shown in Fig. 3, where the C(f) measurements for silicon detectors with various

*This research was supported by the U.S. Department of Energy: Contract No. DE-AC02-76CH00016.

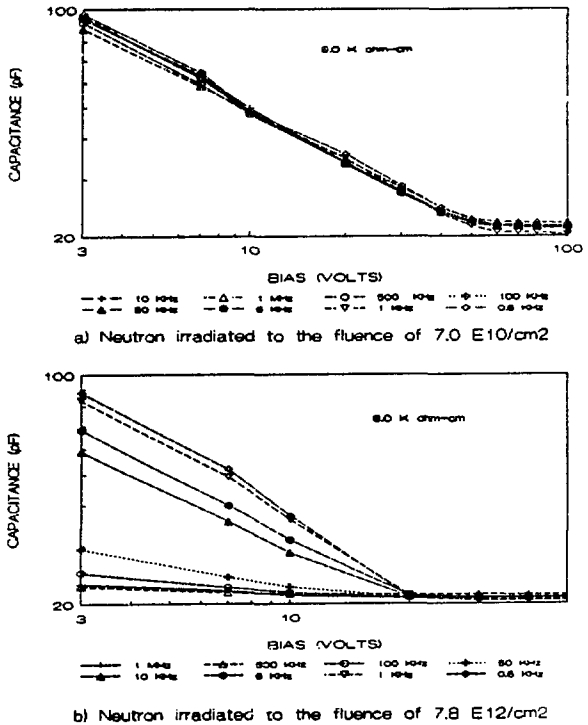

Fig. 1. Detector C-V characteristics at various frequencies of detectors irradiated to the neutron fluence of a) $7.0\times10^{10}/cm^2$, and b) $7.8\times10^{12}/cm^2$.

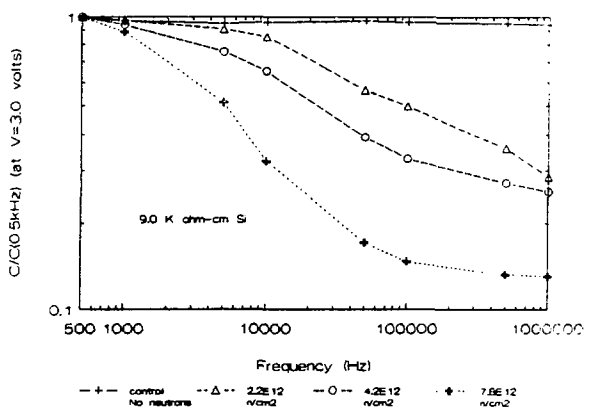

Fig. 2. Data of detector capacitance (at 3.0 V) vs frequency as a function of neutron fluence.

resistivities have been plotted. For the low resistivity silicon detectors, where $N_t/N_d \ll 1$, little or no frequency dependence has been observed.

Modeling

A model describing both the effects of frequency-dependent C-V characteristics and dopant compensation is

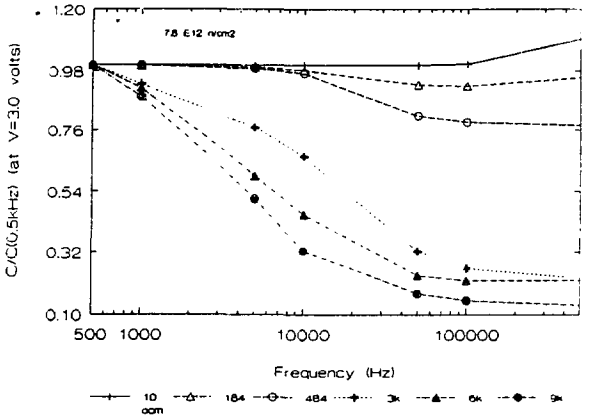

Fig. 3. Data of detector capacitance (at 3.0 V) vs frequency as a function of Si resistivity.

proposed in this study. As it is shown in Fig. 4, two acceptor-like traps are used in this model. Trap level number 1, denoted as E_{t1}, N_{t1}, ϕ_{t1}, etc., is assumed to obey the Fermi-Dirac statistics with the Fermi level being the quasi-fermi level for electrons E_{Fe}, and accounts for the frequency dependence in the model. In the formulism, E_t is the level energy, N is the level concentration, and ϕ_t is the difference between E_t and fermi level (E_F–E_t). The second trap, denoted as E_{t2}, N_{t2}, ϕ_{t2}, etc., as will be described below is assumed to obey the Fermi-Dirac statistics with the Fermi level being the quasi-Fermi level for holes E_{Fh}, and accounts for the dopant compensation [10]. This model is more extensive than the early one proposed by Sah, et al. [6] because it takes into account both the frequency dependence of trap density contributing to capacitance measurement and the effect of dopant compensation. Since all solutions are in their analytical forms, it gives physical insights more clearly than those derived from numerical models [5, 11]. There are other models in the literature that do not explain the effect of voltage-

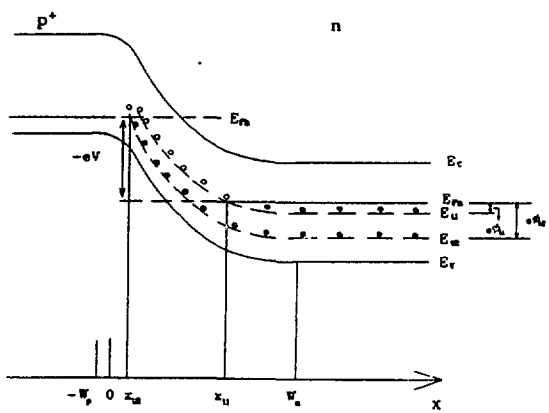

Fig. 4. Energy band diagram for the proposed two-level model describing the observed frequency-dependent C-V effects.

independence of capacitance measured at high frequencies [12-16].

Figure 5 is a schematic of election (e) and hole (h), emission (g), and capture (k) processes between level E_t and the conduction band and the valence band. The capture and emission probabilities per unit time can be written as:

$$k_e = \sigma_e v_e n \tag{1}$$

$$g_e = \sigma_e v_e \gamma n_i e^{[(E_t - E_i)/kT]} \tag{2}$$

$$k_h = \sigma_h v_h p \tag{3}$$

$$g_h = \frac{\sigma_h v_h}{\gamma} n_i e^{[(E_t - E_i)/kT)} \tag{4}$$

Where γ is the level degeneracy, and σ and v are capture cross section and carrier thermal velocity, n_i and E_i are intrinsic carrier density and mid-gap energy, and n and p are electron and hole densities:

$$n = n_i e^{[(E_{Fe} - E_i)/kT]} \tag{5}$$

$$p = n_i e^{[(E_i - E_{Fh})/kT]} \tag{6}$$

here E_{Fe} and E_{Fh} are quasi-Fermi levels for electrons and holes, respectively.

For a deep acceptor-like level ($E_t < E_i$, the second level proposed in the model, E_{t2}) in the band gap (see Fig. 6), if the following statement:

$$\frac{E_t + E_{Fe}}{2} < E_1 \tag{7}$$

where $E_1 \equiv E_i + \frac{kT}{2} \ln\left(\frac{\sigma_h v_h}{\gamma \sigma_e v_e}\right)$ is true, from Eqs. (1), (4), and (5) we will have, in the entire n side of the junction, that:

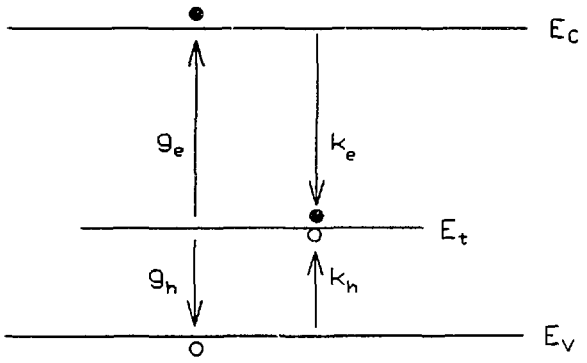

Fig. 5. Schematic of electron and hole capture and emission processes between the level E_t and the conduction and valence bands.

$$g_h \gg k_e \qquad (x \geq 0) \tag{8}$$

As is shown in Fig. 6, in the region of $x > a$, we also have

$$\frac{E_t + E_{Fh}}{2} > E_1 \qquad (x > a) \tag{9}$$

This leads to:

$$\begin{cases} g_e \gg k_h \\ g_h \gg k_e \end{cases} \qquad (x > a) \tag{10}$$

and the level is a generation center.
In a steady state,

$$g_h s = g_e f \tag{11}$$

where s and f are the probabilities of the level being empty and filled with electrons, respectively. Since E_t is assumed to be less than E_i, e.g., $E_t < E_i$, we have

$$\frac{s}{f} = \frac{g_e}{g_h} = \frac{\sigma_e v_e}{\sigma_h v_h} \gamma^2 e^{[(E_t - E_i)/2kT]} \ll 1 \tag{12}$$

and the level in region $x > a$ is filled.

Similarly, in the region of $b < x < a$, since $E_t < E_{Fh}$, we have:

$$\frac{s}{f} = \frac{k_h}{g_h} = \gamma e^{[(E_t - F_{Fh})/kT]} \ll 1 \tag{13}$$

Again the level in region $b < x < a$ is filled, and it is a hole trap. Finally, in region $0 < x < b$, we have $E_t > E_{Fh}$, this leads to

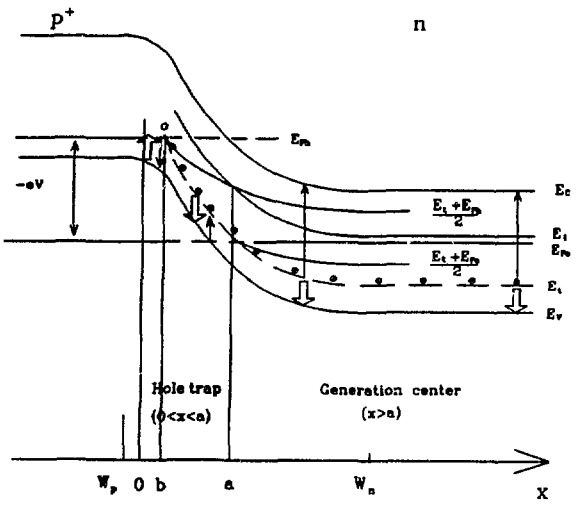

Fig. 6. Illustration of the charge states of a deep acceptor-like center in the band gap. The center is occupied in the majority portion of the junction and acts as a compensation center.

$$\frac{s}{f}=\frac{k_h}{g_h}=\gamma e^{\left[(E_i-E_{Fh})/kT\right]}\gg 1 \tag{14}$$

The level is therefore empty in region $0 < x < b$, and it is again a hole trap. The charge state of the level is also shown in Fig. 6. It is clear that this level is a compensation center that behaves as if it obeys the Fermi-Dirac statistics with the Fermi-level being the quasi-Fermi level for holes.

Using this compensation center (E_{t2}) and another level E_{t1} as is shown in Fig. 4, one can write the Poisson equation as follows:

$$\varepsilon\varepsilon_0\frac{d^2\phi}{dx^2}=\rho(x)=\begin{cases}0 & x\le -W_p\\ -eN_A & -W_p<x\le 0\\ eN_d & 0<x\le x_{t2}\\ eN_d' & x_{t2}<x\le x_{t1}\\ e\left(N_d'-N_{t1}\right) & x_{t1}<x\le W_n\\ 0 & x>W_n\end{cases} \tag{15}$$

Here $N_d' \equiv N_d - N_{t2}$ is the compensated (or effective) dopant density. We can determine W_p,W_n,x_{t1}, and x_{t2} by solving Eq. (15). Since in our case (and in most other cases), $N_d/N_A \le 10^{-7} \ll 1$, we can write, after neglecting terms containing $0(N_d/N_A)$ and $0[(N_d/N_A)^2]$, that:

$$\begin{cases}x_{t2}=\gamma\\ x_{t1}=\gamma+\beta\\ W_n=\alpha+\beta+\gamma\end{cases} \tag{16}$$

where

$$\begin{cases}\alpha=\left(\dfrac{2\varepsilon\varepsilon_0\phi_{t1}}{e\left(N_d'-N_{t1}\right)}\right)^{1/2}\\ \beta=\left(B+\alpha^2\left(1-\dfrac{N_{t1}}{N_d'}\right)^2\right)^{1/2}-\alpha\left(1-\dfrac{N_{t1}}{N_d'}\right)\\ \gamma=\dfrac{1}{1+\dfrac{N_{t2}}{N_d'}}\left[\left(A\left(1+\dfrac{N_{t2}}{N_d'}\right)+\alpha^2\left(1-\dfrac{N_{t1}}{N_d'}\right)^2+B\right)^{1/2}-\right.\\ \qquad\left.-\left(\alpha^2\left(1-\dfrac{N_{t1}}{N_d'}\right)^2+B\right)^{1/2}\right]\\ A=\dfrac{2\varepsilon\varepsilon_0}{eN_d'}\left(V_D-\phi_{t2}\right)\qquad B=\dfrac{2\varepsilon\varepsilon_0}{eN_d'}\left(\phi_{t2}-\phi_{t1}-V\right)\end{cases} \tag{17}$$

Where V_D is the diffusion potential, and V is the applied voltage (V is negative for a reverse bias).

The total charge change in the entire transition region at a given frequency F (or $\omega = 2\pi F$) when a change of applied voltage dV is made to the junction can be written as:

$$dQ = dQ|_{x=x_{t2}} + dQ|_{x=x_{t1}} + dQ|_{x=W_n} \tag{18}$$

$$= q\left[N_{t2}(\omega)\Delta x_{t2} + N_{t1}(\omega)\Delta x_{t1} + \left(N_D - N_{t2} - N_{t1}\right)\Delta W_n\right]$$

and the corresponding voltage change is

$$dV = \frac{q}{\varepsilon\varepsilon_0}\left[N_{t2}(\omega)x_{t2}\Delta x_{t2} + N_{t1}(\omega)x_{t1}\Delta x_{t1} + \right.$$
$$\left. + \left(N_D - N_{t2} - N_{t1}\right)W_n\Delta W_n\right] \tag{19}$$

$N_{t1}(\omega)$ and $N_{t2}(\omega)$ in Eqs. (18) and (19) are frequency dependent defect densities that respond to ac signal with a frequency ω. They are related to equilibrium defect densities N_{t1} and N_{t2} and their corresponding time constants τ_{t1} and τ_{t2} as follows (see Appendix A):

$$N_{t1}(\omega) = \frac{N_{t1}}{1+\omega^2\tau_{t1}^2}$$
$$N_{t2}(\omega) = \frac{N_{t2}}{1+\omega^2\tau_{t2}^2} \tag{20}$$

The frequency-dependent capacitance can then be written as:

$$C(\omega,V) = \frac{dQ}{dV}$$
$$= \varepsilon\varepsilon_0 \frac{N_{t1}(\omega)+N_{t2}(\omega)\dfrac{\Delta x_{t2}}{\Delta x_{t1}} + \left(N_d'-N_{t1}\right)}{N_{t1}(\omega)x_{t1}+N_{t2}(\omega)x_{t2}\dfrac{\Delta x_{t2}}{\Delta x_{t1}} + \left(N_d'-N_{t1}\right)W_n} \tag{21}$$

At high frequencies (HF), i.e., $\omega\tau_{t1}$ and $\omega\tau_{t2} \gg 1$, we have N_{t1} (HF) $\equiv 0$; N_{t2} (HF) $\equiv 0$ and

$$C(V,HF) \equiv \frac{\varepsilon\varepsilon_0}{W_n} \tag{22}$$

From Eqs.(16) and (17) we know that

$$W_n(V) = \left(\frac{2\varepsilon\varepsilon_0\phi_{t1}}{e\left(N_d'-N_{t1}\right)}\right)^{1/2} + \beta(V) + \gamma(V) \tag{23}$$

So if $N_{t1}/N_d' \rightarrow 1$, we have

$$d_{Si} \geq W_n \rightarrow \left(\frac{2\varepsilon\varepsilon_0\phi_{t1}}{e(N_d^+ - N_{t1})}\right)^{1/2} \quad (24)$$

which is voltage independent. Here S_i is the thickness of the Si wafer.
Consequently,

$$C(V,HF) \rightarrow \frac{\varepsilon\varepsilon_0}{d_{Si}} \quad (25)$$

At low frequencies (LF), i.e.,

$$\omega\tau_{t1} \ll 1 \quad (26)$$

since the second level E_{t2} is deep in the lower half of the bandgap, we have,

$$\frac{1}{\tau_{t2}} = e_{n2} \propto e^{[-(E_c - E_{t2})]} \ll e^{[-(E_c - E_{t1})]} \quad (27)$$

or

$$\tau_{t2} \gg \tau_{t1} \quad (28)$$

$\omega\tau_{t2}$ may still satisfy

$$\omega\tau_{t2} \gg 1 \quad (29)$$

From Eq. (20), we have

$$\begin{cases} N_{t1}(LF) \equiv N_{t1} \\ N_{t2}(LF) \equiv 0 \end{cases}$$

and

$$C(V,LF) \equiv \varepsilon\varepsilon_0 \frac{N_d'}{N_{t1}x_{t1} + (N_d' - N_{t1})W_n} \quad (30)$$

Use Eq. (16) we can rewrite Eq. (30) as

$$C(V,LF) \equiv \varepsilon\varepsilon_0 \frac{N_d'}{(N_d' - N_{t1})\alpha + N_d' x_{t1}} \quad (31)$$

At a modestly large bias, say ($-V \geq 3V$), Eq. (31) can be, using Eqs. (10) and (17), approximated as:

$$C(V,LF) \equiv \frac{\varepsilon\varepsilon_0}{\sqrt{\frac{2\varepsilon\varepsilon_0}{eN_d'}(\phi_{t2} - \phi_{t1} - V)}} \quad \text{(for larger biases)} \quad (32)$$

Therefore, at low frequencies, detector capacitance may still behave as $C \propto V^{-1/2}$ at large biases, but the proportional constant now gives the value of the compensated dopant density $N_d' \equiv N_d - N_{t2}$ instead of N_d.

Figure 7 shows $C(V,\omega)$ curves calculated by the model using Eq. (16), Eq. (17) and Eq. (21). A restraint of $d_{Si} \geq W_n \geq 0$ has been used in the calculation. Values of ϕ_{t1} and ϕ_{t2} used in the calculations are 0.2 V and 0.4 V, respectively. Other parameters used in the calculations are listed in the figure. As it is shown in the figure, $C(\omega,V)$ curves predicted by the model are in good agreement with data shown in Figure 1. Figure 8 shows the degree of the C-V frequency dependence as a function of N_{t1}/N_d', while it is demonstrated in Figure 9 that the transition frequency f_t is approximately proportional to the time constant of trap 1, i.e. $f_t \sim 1/\tau_{t1}$.

A good agreement between the experiment data and calculation is illustrated in Figure 10, where calculated C vs. f and data of a p^+n detector with 3 kΩcm resistivity have been plotted. The model predicts that $\tau_{t1} = 4 \times 10^{-5}$ sec in this case.

IV. CONCLUSION

It is concluded that considerable information about the trapping nature of radiation induced defects can be obtained from the frequency dependence of the C(V) characteristics of junction diodes (silicon detectors). Specifically, defect density (N_{t1}) can be determined by the degree of this frequency dependence and the corresponding defect time constant (or electron emission rate $e_n = 1/\tau$) can be obtained from the transition frequency $\tau_{t1} \sim 1/f$ and the compensated dopant density (N_d') can be determined by low frequency C-V measurement of full-depletion voltage (V_d).

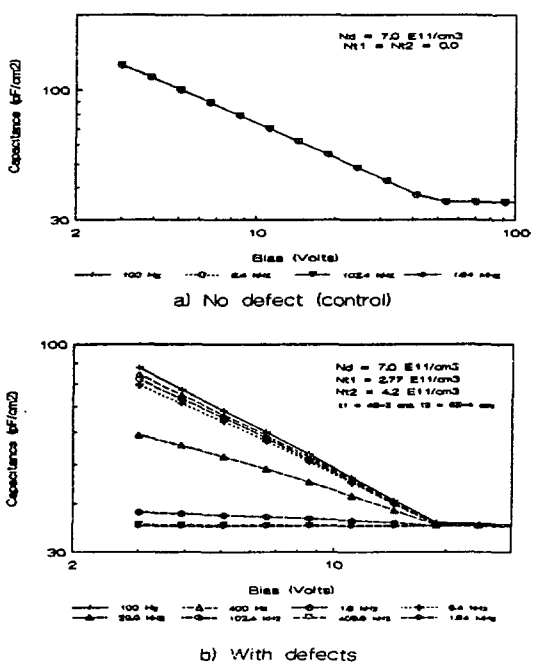

Fig. 7. Calculated frequency-dependent C-V characteristics with a) No defects (control); and b) two defect levels.

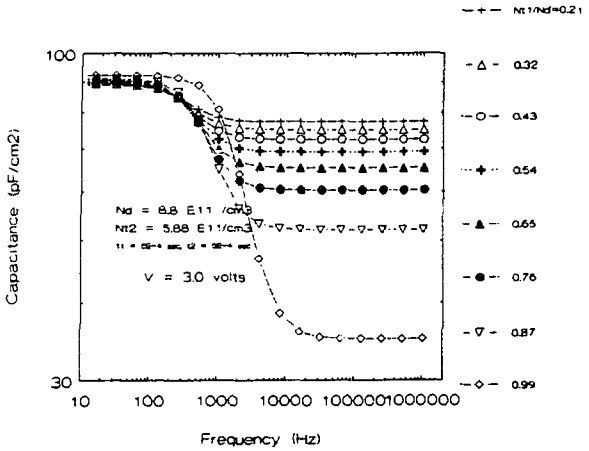

Fig. 8. Calculated C-f plots as a function of N_{t1}/N^{t}_{-d}.

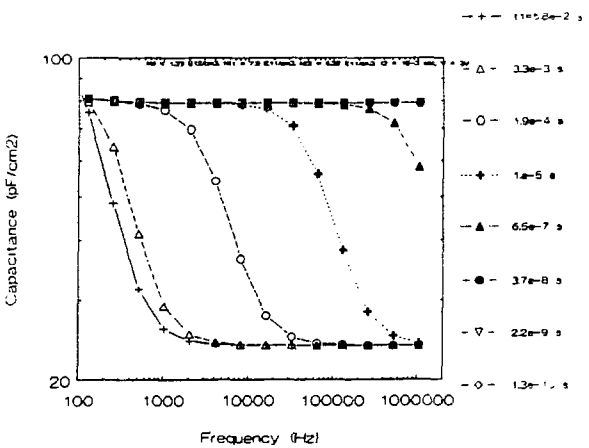

Fig. 9. Calculated C-f plots as a function of τ_{t1}.

V. APPENDIX A
FREQUENCY-DEPENDENT DEFECT DENSITY

For a small change of voltage from

$$V_0 \rightarrow V_0 + \Delta\widetilde{V(t)}$$

where

$$\Delta\widetilde{V(t)} = \Delta V_0 e^{i\omega t} \tag{A1}$$

We have from Eqs. (16) and (17) that

$$\Delta\widetilde{x_t(t)} \propto \Delta\widetilde{V(t)}$$

or

$$\Delta\widetilde{x_t(t)} = \Delta x_t^0 e^{i\omega t} \tag{A2}$$

The total number of traps in $\Delta\widetilde{x_t(t)}$ is

$$\Delta\widetilde{N_T(t)} = N_t \Delta\widetilde{x_t(t)} \bullet \text{Area} \equiv \Delta N_t^0 e^{i\omega t} \tag{A3}$$

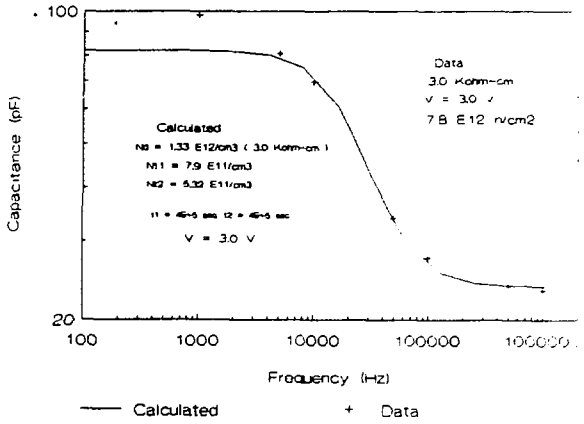

Fig. 10. Comparison between calculated and measured C-f data.

The rate equation for charges in $\Delta\widetilde{x_t(t)}$ that are emitted to conduction band (or detrapped) and contributes to the capacitance, $\Delta\widetilde{N(t)}$, is

$$\frac{d\Delta\widetilde{N(t)}}{dt} = e_n\left[\Delta\widetilde{N_T(t)} - \Delta\widetilde{N(t)}\right] \tag{A4}$$

Where e_n is the electron emission coefficient.
Solution of Eq. (A4) is

$$\Delta\widetilde{N(t)} = \Delta N_t^0 \frac{e_n}{e_n + i\omega}\left[e^{i\omega t} - e^{-e_n t}\right] \tag{A5}$$

For a measurement time longer than $1/e_n$, or for $t \gg 1/e_n$,

$$\Delta\widetilde{N(t)} = \Delta N_t^0 \frac{e_n}{e_n + i\omega} e^{i\omega t} \tag{A6}$$

Or using Eq. (A3):

$$\Delta\widetilde{N(t)} = N_t \Delta\widetilde{x_t(t)} \bullet \text{Area} \bullet \frac{1}{1+i\omega\tau} \tag{A7}$$

Where $\tau = 1/e_n$ is the time constant.

The density of charges emitted to conduction band and therefore contributing to the capacitance is then:

$$\widetilde{N_t(\omega)} = \frac{\Delta\widetilde{N(t)}}{\Delta\widetilde{x_1(t)} \bullet \text{Area}} = \frac{N_t}{1+i\omega\tau} \tag{A8}$$

take the real part, we finally obtain:

$$N_t(\omega) = \frac{N_t}{1+\omega^2\tau^2} \tag{A9}$$

VI. REFERENCE

[1] H. W. Kraner, Z. Li and K. V. Posnecker, "Fast Neutron Damage in Silicon Detectors," *Nucl. Instrum. Methods*, A279, 266 (1989).

[2] G. Lindstrom, E. Fretwurst, H. Herdan, M. Rollwagen P. Thomsen, and R. Wunstorf, "Radiation Damage Effects in Silicon Detectors," DESY 89-105, August (1989).

[3] H. Dietl, T. Gooch, D. Kelsey, R. Klanner, A. Loffler, M. Pepe, and F. Wickens, "Radiation Damage in Silicon Strip Detectors," *Nucl. Instrum. Methods*, **A235**, 460 (1987).

[4] H. W. Kraner, "Radiation Damage in Silicon Detectors," *Nucl. Instrum. Methods*, **225**, 615 (1984).

[5] C. W. Gwyn, "Calculated Small Signal Characteristics for Irradiated PN Junctions," *IEEE Trans. Nucl. Sci.*, **NS-19**, 355 (1972).

[6] C. T. Sah and V. C. K. Redd, "Frequency Dependence of Reverse Biased Capacitance of Gold-doped Silicon P^+N Step Junctions," *IEEE Trans. on Electron Devices*, **ED-16**, 345 (1969).

[7] H. W. Kraner, Richard H. Pehl and E. E. Haller, "Fast Neutron Radiation Damage of High Purity Germanium Detectors," *IEEE Trans. Nucl. Sci.*, **NS-22**, 149 (1975).

[8] "Radiation Levels in the SSC Interaction Regions," Task Force Report, D. E. Groom, Editor, SSC-SR-1033 (1989).

[9] L. Vismara, "SICAPO Collaboration: Radiation Damage Effects on Silicon Detectors," Paper presented at the Intl. Conf. on Advanced Technology and Particle Physics, Como, Italy, 13-16 June 1988.

[10] "Point Defects in Semiconductors," J. Bourgoin and M. Lannoo, Vol. 2, Springer- Verlag, New York, p. 154-162 (1983).

[11] E. P. Eernisse, "Accurate Capacitance Calculations for PN Junction Containing Traps," *J. Appl. Phys. Letters*, **18**, No. 5, 183 (1973).

[12] Y. Zohta, "Frequency Response of Gold Impurity Centers in the Depletion Layer of Reverse-biased Silicon P^+–n Junctions," *J. Appl. Phys.*, **43**, No. 4, 1713 (1972).

[13] Y. Zohta and Y. Ohmura, "Determination of the Sparial Distribution of Deep Centers from Capacitance Measurements of PN Junctions," *Appl. Phys. Lett.*, **21**, No. 3, 117 (1972).

[14] G. Vincent, D. Bois, and P. Pinard, "Conductance and Capacitance Studies in Gap Schottky," *J. Appl. Phys.*, **46**, No. 12, 5173 (1975).

[15] Y. Tokuka and A. Usami, "Admittance Studies of Neutron-Irradiated Silicon P^+–n Diodes," *J. Appl. Phys.*, **48**, No. 4, 1668 (1977).

[16] Y. Tokuda and A. Usami, "Studies of Defects in Neutron-Irradiated P-type Silicon by Admittance Measurements of n^+–p Diodes," *J. Appl. Phys.*, **49**, No. 2, 603 (1978).